Stanford Exploration Project, Report 92, November 12, 1997, pages 91–108

Fluid-flow simulation concept of methane hydrate growth and decomposition

Christine Ecker[1]

keywords: *gas, phase, permeability*

ABSTRACT

Bottom simulating reflectors (BSR) are associated with the base of the stability zone of methane hydrates. The occurrence, stability and breakdown of these BSRs is considerably dependent on the temperature and pressure conditions in the sediment. Any P-T changes can affect the hydrate stability significantly and thus influence the behavior of the BSRs. I present the theory and development of a three-dimensional finite-difference fluid-flow simulator for hydrate decomposition/growth in porous media. I derive the equation for a 3-phase/2-component isothermal gas-water-hydrate system and discuss the code development of a two-dimensional system. The code is still in a test phase and is not working properly for all required cases. I show the results of some preliminary code testing based on simple gas-water flow. Furthermore, I discuss how to include more realistic thermodynamics into the system.

INTRODUCTION

Methane hydrate structures are increasingly recognized as potential energy resources due to the significant amount of fuel energy tied up in them (Kvenvolden, 1993). Furthermore, they might have a significant contribution to the methane balance in the atmosphere, thus affecting global climate and buffering its change. Therefore, knowledge of the reservoir properties of methane hydrate, such as the amount of hydrate present, its mobility and recoverability, is essential. The means of seismic detection and characterization is provided by bottom simulating reflectors (BSRs), which mark the bottom of the stability zone of methane hydrates. Since hydrates are stable only in a certain pressure-temperature regime, limited information is available from deep sea drilling (Kvenvolden and Barnard, 1983; MacKay et al., 1994; Dallimore and Collett, 1995) and most information regarding the elastic properties is inferred directly from the seismic reflection data (Singh et al., 1993; Katzman et al., 1994; Ecker and Lumley, 1994). Since the recognition of hydrate structures in seismic data

[1]**email:** christin@sep.stanford.edu

is primarily dependent on the presence of BSRs, the understanding of their formation, stability and breakdown is essential.

As the base of the hydrate stability zone, BSRs are highly dependent on the pressure-temperature regime in shallow marine sediments. Changes in sea-level, mass slides, diapirs, etc. can have a considerable impact on these regimes, possibly causing hydrate decomposition or growth, and thus resulting in possible breakdown or reformation of the BSRs (Dillon et al., 1993). This could explain the deformation and discontinuities in the BSRs often visible in seismic sections. Fluid-flow simulation of the change of hydrate structures under certain pressure/temperature perturbation can give a good first-order insight into the BSR behavior coupled with it.

Information about kinetic hydrate decomposition and growth is available from several laboratory measurements (Kim et al., 1987; Englezos et al., 1987; Yousif et al., 1991). Furthermore, several 1-D simulations have been conducted on the dissociation of methane hydrate to investigate possible schemes of gas recovery from the hydrate structures (Verigin et al., 1980; Bondarev et al., 1989; Jamaluddin et al., 1989; Yousif et al., 1991). Little work, however, has been done in directly trying to simulate the changes in BSR occurrence coupled with pressure/temperature perturbations and, subsequently, relating it to real seismic observations.

In this paper, I present the theory and development of a three-dimensional finite-difference fluid-flow simulator for hydrate growth and decomposition in porous media. I show the fluid equations for the 3-phase/2-component gas-water-hydrate system based on the conservation of mass and discuss the code development based on those equations. In this first phase of the simulation attempt, the system is considered to be completely isothermal and the thermodynamic effects are not yet been taken into account. A more realistic flow system based on heat transfer can be formulated using an equation of energy balance and can be added once the isothermal model has been sufficiently tested. The code is still in a testing phase and does not work properly for all required cases. I show the preliminary results of some code testing based on simple gas-water flow. The hydrate simulation itself requires more work in order to obtain a working program. Finally, I discuss how the code could be extended to include the thermodynamics of the system.

METHANE HYDRATE STABILITY AND BREAKDOWN

Methane hydrate is a substance in which the molecules of gas and water chemically interact to form an ice-like crystalline structure. This structure is stable within a certain pressure-temperature regime. The phase diagram in Figure 1 shows clearly that this pressure-temperature regime requires either low pressure/low temperature or high pressure/high temperature. Associated with the base of the hydrate stability field are bottom simulating reflectors (BSRs) that parallel the seafloor at a subbottom depth of several hundred meters. Seismic reflection profiles often show a discontinuous or fading behavior of these BSRs (Figure 2), which might be explained by perturba-

tions in the pressure-temperature profile in the shallow marine sediments. Changes in the pressure and temperature will ultimately affect the position and characteristic of the BSR since it will result in different hydrate stability conditions.

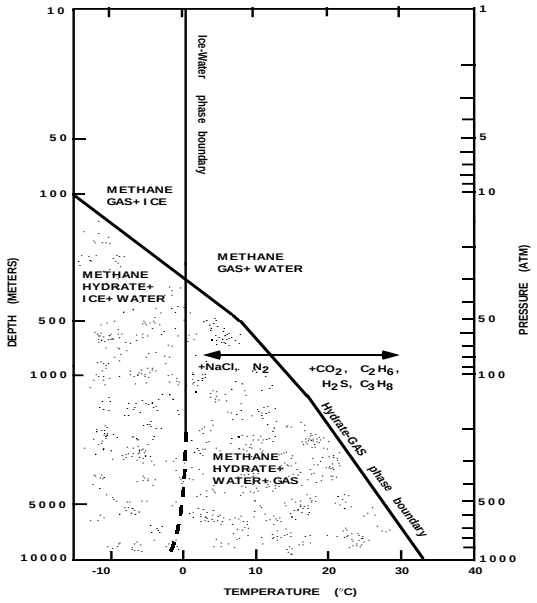

Figure 1: Phase diagram showing the boundary between methane gas and methane hydrate. Redrawn after Kvenvolden (1993). christin1-phase [NR]

Several possible scenarios that can cause such pressure/temperature perturbations can be imagined, such as changes in sea level, land slides, faults and diapirs, etc.. Figure 3 illustrates the cases of sea level fall and mass sliding. In both events, pressure reduction and temperature will affect the hydrate stability field, placing the BSR into a zone of hydrate instability. This will result in the breakdown of the hydrate and, consequently, in a change of the BSR. While the BSR will be affected on a global scale in case of sea level fall, mass slides will have a more local effect on the BSRs. In order to understand and successfully characterize seismic sections showing discontinuous, fading BSRs, we must have knowledge of the behavior of the BSRs under hydrate breakdown. Moreover, several crucial questions related to this breakdown must be answered if we are to characterize the hydrate structures. How will this breakdown affect the BSR? Will the BSR disappear and rebuild in the new hydrate stability zone? If so, how long would it take to be rebuilt? Is there still hydrate, even though there is no longer a BSR? What will happen to the gas that will be released from the dissociating hydrate? Will it migrate upwards undisturbed, or will it form hydrate again? Fluid-flow simulation of a disturbed hydrate zone should be a good way to get a first-order insight into these questions. It should enable me to anticipate the changes in hydrate structure and BSR.

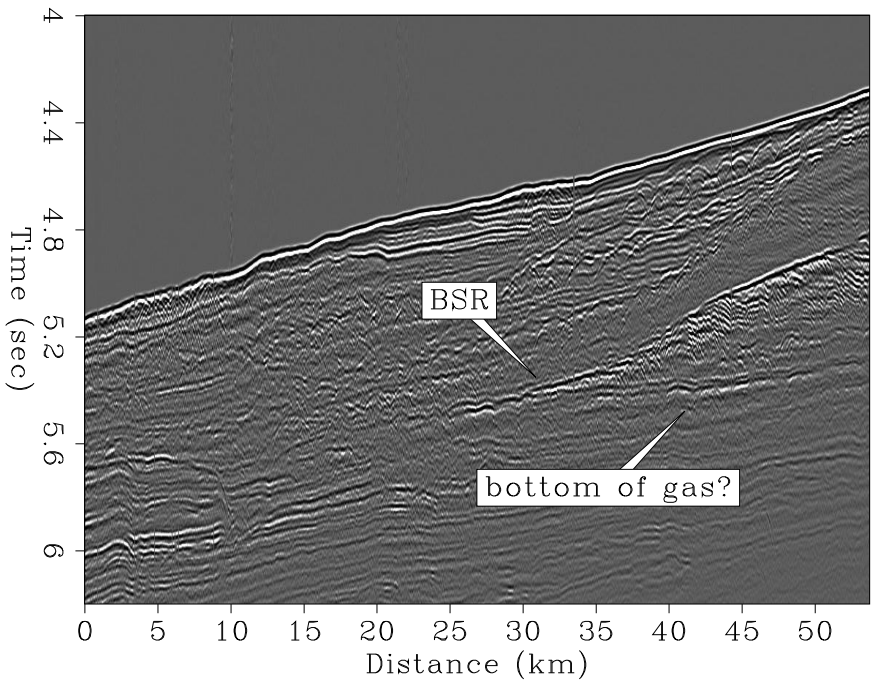

Figure 2: Near-offset stack section of data from the Blake Outer Ridge, offshore Florida and Georgia, showing a discontinuous BSR. christin1-near-ann [NR]

FLUID-FLOW SIMULATION

Concept of flow simulation

Fluid flow of a dissociating or growing hydrate structure can be modeled as a three-phase, two-component flow system. The three phases are gas, water and hydrate, and the two components are gas and water. Only gas and water are flowing phases; hydrate is a solid phase. Pressure reduction of a stable hydrate structure will result in gas production from the dissociating hydrate, thus stimulating fluid flow as a function of time t. The flow of gas and water through a hydrate stability zone, on the other hand, will result in the simulation of hydrate growth. In this first attempt at hydrate simulation, I assume that the system can be modeled under isothermal conditions; thus, only pressure effects are accounted for and any change of temperature will be neglected. In reality, to model such complicated systems as hydrate structures is not a valid assumption. However, it is the most simple model of the problem upon which the more complicated thermodynamic system can be built. Thus the isothermal flow simulation is the base for the thermal flow simulation. The isothermal flow of the system can be approximated by coupling fluid-mass conservation with Darcy's law which relates a gradient in pore pressure P and gravity to the rate of fluid flow. The

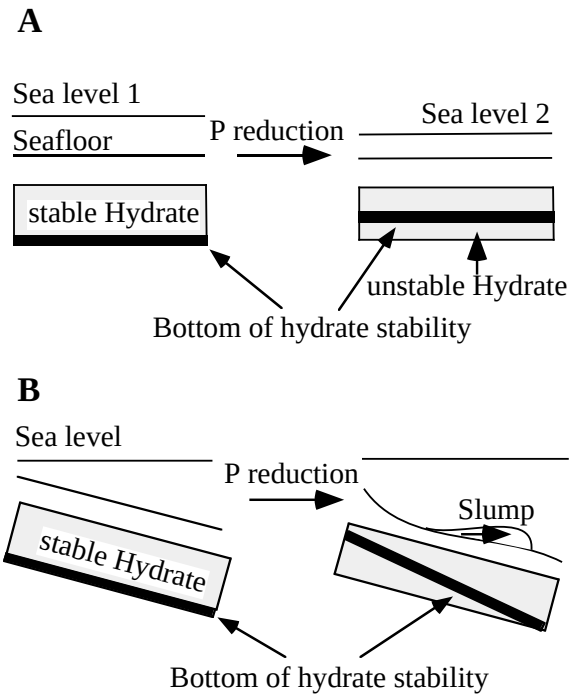

Figure 3: Illustration of hydrate breakdown. The upper part illustrates the change in the hydrate stability due to a drop in sea level thus affecting the BSR on a global scale. The lower part displays the stability behavior for mass slides which affects BSRs on a local scale. christin1-break [NR]

law of mass conservation can be expressed as

$$\begin{pmatrix} Rate\ of \\ accumulation \end{pmatrix} = \begin{pmatrix} Rate \\ transported\ in \end{pmatrix} - \begin{pmatrix} Rate \\ transported\ out \end{pmatrix} + \begin{pmatrix} Rate\ of \\ production \end{pmatrix}$$

Following this equation of mass conservation, the fluid-flow equations for the gas phase, water phase, and hydrate phase are:

$$\frac{\partial}{\partial t}(\phi\rho_g S_g + \phi\rho_w S_w X_{g,w} + \phi\rho_h S_h X_{g,h}) = \nabla(v_g\rho_g + v_w\rho_w X_{g,w}) + \dot{m}_g, \tag{1}$$

$$\frac{\partial}{\partial t}(\phi\rho_w S_w X_{w,w} + \phi\rho_h S_h X_{w,h}) = \nabla(v_w\rho_w X_{w,w}) + \dot{m}_w, \tag{2}$$

$$\frac{\partial}{\partial t}(\phi\rho_h S_h) = -\dot{m}_h. \tag{3}$$

The subscripts g, w, and h stand for gas, water, and hydrate, respectively. The porosity of the system is denoted by ϕ, the density of the i-th phase by ρ_i, and the saturation of the i-th phase in the pore space by S_i, which varies on a scale from zero to unity. The density of the gas and water phases are pressure and temperature dependent ($\rho_g(P,T)$, $\rho_w(P,T)$), thus incorporating expansion and compression effects under variable pressure-temperature conditions. The density of hydrate is constant. The mass fraction of component c in phase i is denoted by $X_{c,i}$ ($X_{g,w}$ is the mass fraction of gas in water, $X_{w,w}$ the mass fraction of water in water, etc.). These mass fractions can also change as a function of pressure and temperature $X_{c,i}(P,T)$). The gas and water phase have a velocity of v_g and v_w. The gas production/depletion rate is included as $\dot{m}_g$, the water production/depletion rate as $\dot{m}_w$, and the hydrate dissociation/growth rate as $\dot{m}_h$. These source/sink terms are related by (Yousif et al., 1991):

$$\dot{m}_h = \dot{m}_g + \dot{m}_w, \tag{4}$$

$$\dot{m}_g = \dot{m}_h \frac{M_g}{N_h M_w + M_g} \tag{5}$$

where M_g and M_w are the mole weights of gas and water, and N_h is the hydrate number. The local gas generation/depletion rate caused by hydrate dissociation or growth can be obtained by the Kim-Bishnoi model (Kim et al., 1987) and the Englezos model (Englezos et al., 1987):

$$\dot{m}_g = K_{d/g} A_s (P_e(T) - P) \tag{6}$$

where $K_{d/g}$ is a constant characterizing either hydrate dissociation or growth. The specific surface area of the pore volume occupied by gas and water is A_s, and $P_e(T)$

is the equilibrium pressure of hydrate for a certain temperature T. Equation (6) is a kinematic model which is only valid for sufficiently small pressures and temperatures. Given the equilibrium pressure for hydrates at different temperatures, this formula results in the gas production/depletion rates depending on pressure-temperature fields.

The flow-equations (1), (2), and (3) are coupled with Darcy's law:

$$v_g = -\kappa_{abs}\frac{\kappa_{rg}}{\mu_g}(\nabla P - \rho_g g \nabla z), \tag{7}$$

$$v_w = -\kappa_{abs}\frac{\kappa_{rw}}{\mu_w}(\nabla P - \rho_w g \nabla z) \tag{8}$$

which relates the velocities of gas and water (v_g and v_w) to the absolute permeability κ_{abs}, the relative permeability of gas and water κ_{rg} and κ_{rw}, the gradient in pore pressure P and the gravity effect. The viscosities of water and gas are denoted by μ_w and μ_g. In this first simulation attempt, the capillary pressure has been neglected; I thus assume the same pore pressure for gas and water. The absolute permeability is a function of hydrate saturation ($K_{abs}(S_h)$), dependent on the deposition of the hydrate in the pore space (Ecker et al., 1995).

For solving the flow system, the following conditions have to be satisfied:

$$S_g + S_w + S_h = 1, \tag{9}$$

$$X_{g,w} + X_{w,w} = 1, \tag{10}$$

$$X_{g,h} + X_{w,h} = 1. \tag{11}$$

Combining equations (1), (2), and (3) with equations (7) to (11) results in

$$\begin{aligned}&\tfrac{\partial}{\partial t}(\phi\rho_g S_g + \phi\rho_w(1 - S_g - S_h)X_{g,w} + \phi\rho_h S_h X_{g,h})\\ &= \nabla(-\kappa_{abs}\frac{\kappa_{rg}}{\mu_g}\rho_g(\nabla P - \rho_g g\nabla z) - \kappa_{abs}\frac{\kappa_{rw}}{\mu_w}\rho_w X_{g,w}(\nabla P - \rho_w g\nabla z)) + \dot{m}_g,\end{aligned} \tag{12}$$

$$\begin{aligned}&\tfrac{\partial}{\partial t}(\phi\rho_w(1 - S_g - S_h)(1 - X_{g,w}) + \phi\rho_h S_h(1 - X_{g,h}))\\ &= \nabla(-\kappa_{abs}\frac{\kappa_{rw}}{\mu_w}\rho_w(1 - X_{g,w})(\nabla P - \rho_w g\nabla z)) + \dot{m}_w,\end{aligned} \tag{13}$$

$$\frac{\partial}{\partial t}(\phi\rho_h S_h) = -\dot{m}_h. \tag{14}$$

Equations (9) through (14) describe the fluid flow of the three phase/ two component gas-water-hydrate system caused by either hydrate dissociation or hydrate growth. The unknowns are pore pressure P and two saturations, in this case gas and hydrate saturation.

Finite-difference formulation

The equations that govern the fluid flow through a porous medium can be solved numerically using a finite-difference method. For three dimensions, the finite difference approximations of equation (12) through (14) can be written as

$$\frac{V_{ijk}}{\Delta t}\Delta_t(\phi\rho_g S_g+\phi\rho_w(1-S_g-S_h)X_{g,w}+\phi\rho_h S_h X_{g,h})_{ijk} = [(\Delta T_g\rho_g\Delta P)_i-(\Delta T_g{\rho_g}^2 g\Delta z)_i$$

$$+(\Delta T_w\rho_w X_{g,w}\Delta P)_i - (\Delta T_w{\rho_w}^2 X_{g,w}g\Delta z)_i] + [(\Delta T_g\rho_g\Delta P)_j - (\Delta T_g{\rho_g}^2 g\Delta z)_j$$

$$+(\Delta T_w\rho_w X_{g,w}\Delta P)_j - (\Delta T_w{\rho_w}^2 X_{g,w}g\Delta z)_j] + [(\Delta T_g\rho_g\Delta P)_k - (\Delta T_g{\rho_g}^2 g\Delta z)_k$$

$$+(\Delta T_w\rho_w X_{g,w}\Delta P)_k - (\Delta T_w{\rho_w}^2 X_{g,w}g\Delta z)_k] + \dot{m}_{g_{ijk}}, \tag{15}$$

$$\frac{V_{ijk}}{\Delta t}\Delta_t\left(\phi\rho_w(1-S_g-S_h)(1-X_{g,w})+\phi\rho_h S_h(1-X_{g,h})\right)_{ijk} = [(\Delta T_w\rho_w(1-X_{g,w})\Delta P)_i$$

$$-(\Delta T_w{\rho_w}^2(1-X_{g,w})g\Delta z)_i]+[(\Delta T_w\rho_w(1-X_{g,w})\Delta P)_j-(\Delta T_w{\rho_w}^2(1-X_{g,w})g\Delta z)_j]$$

$$+[(\Delta T_w\rho_w(1-X_{g,w})\Delta P)_k - (\Delta T_w{\rho_w}^2(1-X_{g,w})g\Delta z)_k] + \dot{m}_{w_{ijk}}, \tag{16}$$

$$\frac{V_{ijk}}{\Delta t}\Delta_t\left(\phi\rho_h S_h\right)_{ijk} = -\dot{m}_{h_{ijk}} \tag{17}$$

where V_{ijk} is the grid block volume and

$$T_g = \frac{A}{\Delta d}\kappa_{abs}\frac{\kappa_{rg}}{\mu_g}, \tag{18}$$

$$T_w = \frac{A}{\Delta d}\kappa_{abs}\frac{\kappa_{rw}}{\mu_w}. \tag{19}$$

are the gas and water transmissibilities. The cross-sectional area normal to the direction of the flow at the block-boundary is denoted by A, and the distance between two connecting grid points by Δd.

The accumulation terms in equations (15) to (17) are given as

$$\begin{aligned}&\Delta_t\left(\phi\rho_g S_g+\phi\rho_w(1-S_g-S_h)X_{g,w}+\phi\rho_h S_h X_{g,h}\right)_{ijk}\\&=\left(\phi\rho_g S_g+\phi\rho_w(1-S_g-S_h)X_{g,w}+\phi\rho_h S_h X_{g,h}\right)_{ijk}^{t+1}\\&-\left(\phi\rho_g S_g+\phi\rho_w(1-S_g-S_h)X_{g,w}+\phi\rho_h S_h X_{g,h}\right)_{ijk}^{t},\end{aligned} \tag{20}$$

$$\begin{aligned}&\Delta_t\,(\phi\rho_w(1-S_g-S_h)(1-X_{g,w})+\phi\rho_h S_h(1-X_{g,h}))_{ijk}\\&=(\phi\rho_w(1-S_g-S_h)(1-X_{g,w})+\phi\rho_h S_h(1-X_{g,h}))^{t+1}_{ijk}\\&-(\phi\rho_w(1-S_g-S_h)(1-X_{g,w})+\phi\rho_h S_h(1-X_{g,h}))^{t}_{ijk},\end{aligned}\tag{21}$$

$$\Delta_t\,(\phi\rho_h S_h)_{ijk}=(\phi\rho_h S_h)^{t+1}_{ijk}-(\phi\rho_h S_h)^{t}_{ijk}.\tag{22}$$

The finite-difference operators in equations (15) to (17) are given by

$$(\Delta T_g\rho_g\Delta P)_l=T_{g_{l+\frac{1}{2}}}\rho_{g_{l+\frac{1}{2}}}(P_{l+1}-P_l)-T_{g_{l-\frac{1}{2}}}\rho_{g_{l-\frac{1}{2}}}(P_l-P_{l-1}),\tag{23}$$

$$(\Delta T_g{\rho_g}^2 g\Delta z)_l=T_{g_{l+\frac{1}{2}}}\rho^2_{g_{l+\frac{1}{2}}}g(z_{l+1}-z_l)-T_{g_{l-\frac{1}{2}}}\rho^2_{g_{l-\frac{1}{2}}}g(z_l-z_{l-1}),\tag{24}$$

$$(\Delta T_w\lambda_w\Delta P)_l=T_{w_{l+\frac{1}{2}}}\lambda_{w_{l+\frac{1}{2}}}(P_{l+1}-P_l)-T_{w_{l-\frac{1}{2}}}\lambda_{w_{l-\frac{1}{2}}}(P_l-P_{l-1}),\tag{25}$$

$$(\Delta T_w\Gamma_w g\Delta z)_l=T_{w_{l+\frac{1}{2}}}\Gamma_{w_{l+\frac{1}{2}}}g(z_{l+1}-z_l)-T_{w_{l-\frac{1}{2}}}\Gamma_{w_{l-\frac{1}{2}}}g(z_l-z_{l-1})\tag{26}$$

where subscript $l=i,j,k$ and
$\lambda_w=\rho_w X_{g,w}$ for equation (15),
$\lambda_w=\rho_w(1-X_{g,w})$ for equation (16),
$\Gamma_w={\rho_w}^2 X_{g,w}$ for equation (15) and
$\Gamma_w={\rho_w}^2(1-X_{g,w})$ for equation (16).

Furthermore, it is:

$$T_{g_{l+\frac{1}{2}}}=\frac{A_{l+\frac{1}{2}}}{\Delta d_l}(\kappa_{abs}\frac{\kappa_{rg}}{\mu_g})_{l+\frac{1}{2}},\tag{27}$$

$$T_{w_{l+\frac{1}{2}}}=\frac{A_{l+\frac{1}{2}}}{\Delta d_l}(\kappa_{abs}\frac{\kappa_{rw}}{\mu_w})_{l+\frac{1}{2}}\tag{28}$$

where $A_{l+\frac{1}{2}}$ is the cross-sectional area normal to the direction of the flow at the block-boundary $l+\frac{1}{2}$. The distance between grid points l and $l+1$ is given by Δd_j. The absolute permeability is taken in the direction of the flow.

Equations (20) to (28) use coefficients that must be evaluated at intercell boundaries between two grid points. Simple arithmetic mean is used to approximate the densities ρ_g, ρ_w, and ρ_h, and the mass fractions $X_{g,w}$ and $X_{g,h}$. The absolute permeability κ_{abs} as a function of S_h is determined using harmonic weighting. Upstream

weighting is used for the relative relative permeabilities and viscosities. Defining the phase potential as

$$\Phi_p = P_p - \rho_p g h \tag{29}$$

where the subscript p represents either gas phase g or water phase w, upstream weighting means:

$$\Phi_{p_l} > \Phi_{p_{l-1}} \longrightarrow (\tfrac{\kappa_{rp}}{\mu_p})_{l-\frac{1}{2}} = (\tfrac{\kappa_{rp}}{\mu_p})_l$$

$$\Phi_{p_l} < \Phi_{p_{l-1}} \longrightarrow (\tfrac{\kappa_{rp}}{\mu_p})_{l-\frac{1}{2}} = (\tfrac{\kappa_{rp}}{\mu_p})_{l-1}$$

Equations (15) to (28) represent the finite-difference set-up for a three-dimensional fluid-flow simulator of a gas-water-hydrate system, which can be solved using the Newton-Raphson method.

Code implementation and testing

The actual program has been coded for a two-dimensional system, but can easily be extended to three dimensions, as the equations have shown. All equations are solved implicitly for the pore pressure P, the gas saturation S_g and the hydrate saturation S_h at each grid point with the Newton-Raphson method using a Cartesian grid system. A flow chart of the code can be seen in Figure 4.

The time is denoted by n, the number of Newton iterations by it, and the time steps by Δt. Each new Δt is calculated automatically based on the following relationship (Aziz, 1995):

$$\Delta t^{n+1} = \Delta t^n \left(\frac{(1+\omega)\eta_{ijk}}{\delta_{ijk} + \omega\eta_{ijk}} \right)_{min_{over_{ijk}}} \tag{30}$$

The desired change of either pore pressure P or saturations S_g and S_h over Δt^n is given by η_{ijk}, the actual change by δ_{ijk} and ω is a tuning factor with values between zero and unity. Usually, η_{ijk} has the same value for all grid blocks, but different values for the different variables (in this case, pressure P, gas and hydrate saturation S_g and S_h). So a different Δt^{n+1} is calculated for each variable and the minimum is used for the subsequent time step.

Initially, the system is characterized by a given pore pressure, temperature, gas and hydrate saturation. Perturbation of the pressure at time $t = 0$ or an initial system, which is not in equilibrium, will initialize fluid-flow through the system. The boundary conditions depend on the initial system, and assume either constant pressure boundary at $z = 0$ and no-flow boundaries everywhere else, or no-flow boundaries everywhere.

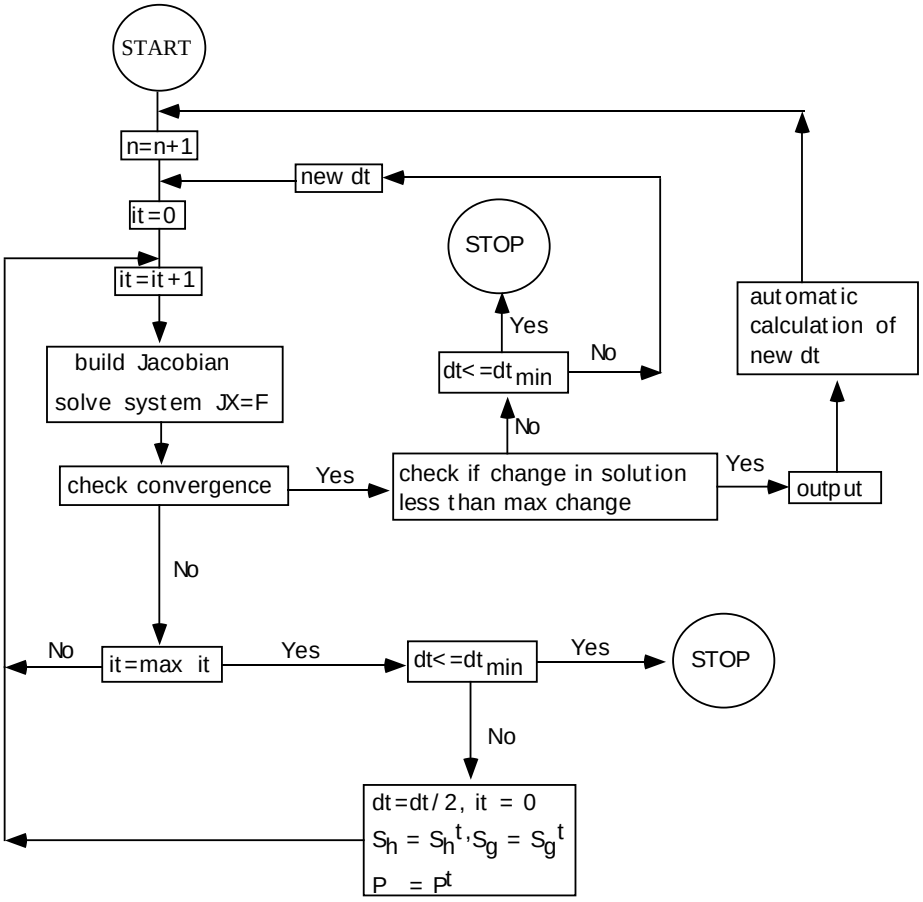

Figure 4: Flow chart of the simulation code. christin1-flow [NR]

The code is still in a test phase. As of now, it is working for only two-phase flow and such small hydrate saturation that neither hydrate growth nor dissociation can occur. It is still unstable and non-converging for hydrate saturations bigger than 0.01. Additional work is required to correct this problem.

I conducted a simple test on the functionality of the code for at least two-phase fluid flow with the third, solid hydrate phase being approximately zero. The initial system consisted of a no-flow boundary setup of water over gas with a negligible small hydrate saturation everywhere. The initial pore pressure was comparable to hydrostatic pressure, and the temperature was chosen so that neither hydrate growth nor decomposition could be expected for the pore pressure range. The density difference of gas and water, the pressure gradient and the effect of gravity result in a fluid flow stimulation in which the gas migrates upward and the water travels down.

The grid system is a 10x10 system, each grid block having dimensions of 10 m x 10 m. The top of the grid system is at about 1000 m depth. The grid blocks within the first 40 m are filled with 100% water, the last 60 m are filled with 100% gas. To avoid any instabilities resulting from a vanishing third flow equation (hydrate equation), a constant hydrate saturation of 0.001 was assumed throughout the system. The temperature was chosen to be 10 degrees, and the initial pore pressure followed the relation $P_{ij} = 1000$ kg/cm $*9.81$ m$/s^2$ $*z_{ij}$. The viscosities were assumed to be constant with $\mu_g = 0.4$ cp and $\mu_w = 1.0$ cp. The relative permeabilities were simply expressed by $\kappa_{rg} = s_g^2$ and $\kappa_{rw} = (1 - S_g - S_h)^2$. The densities were assumed to be slightly compressible with $\rho_g = 0.006 + p/10^5$ and $\rho_w = 1.0 + p/10^4$. The absolute permeability was a random permeability field with values between 10 mD and 10000 mD for each grid block.

Figure 5 shows the gas saturation results of the fluid-flow initialized by the instable gas-water system. 100 % gas saturation is displayed as white, 0 % as black. At time 0, the water is above the gas and fluid flow is stimulated. After 1 day, gas and water have started to migrate depending on low and high permeabilities in the different grid blocks. Following the permeability pattern, the two fluids begin to mix. After 155 days, the two phases have nearly equilibrized and finally they reach their equilibrium state with gas above water. As soon as this equilibrium state is reached, there is no more flow through the system.

The test shows that the code appears to work correctly for at least a two-phase fluid flow. More work is still required to improve upon the incorporation of a third-phase with more than 0.001 saturation everywhere.

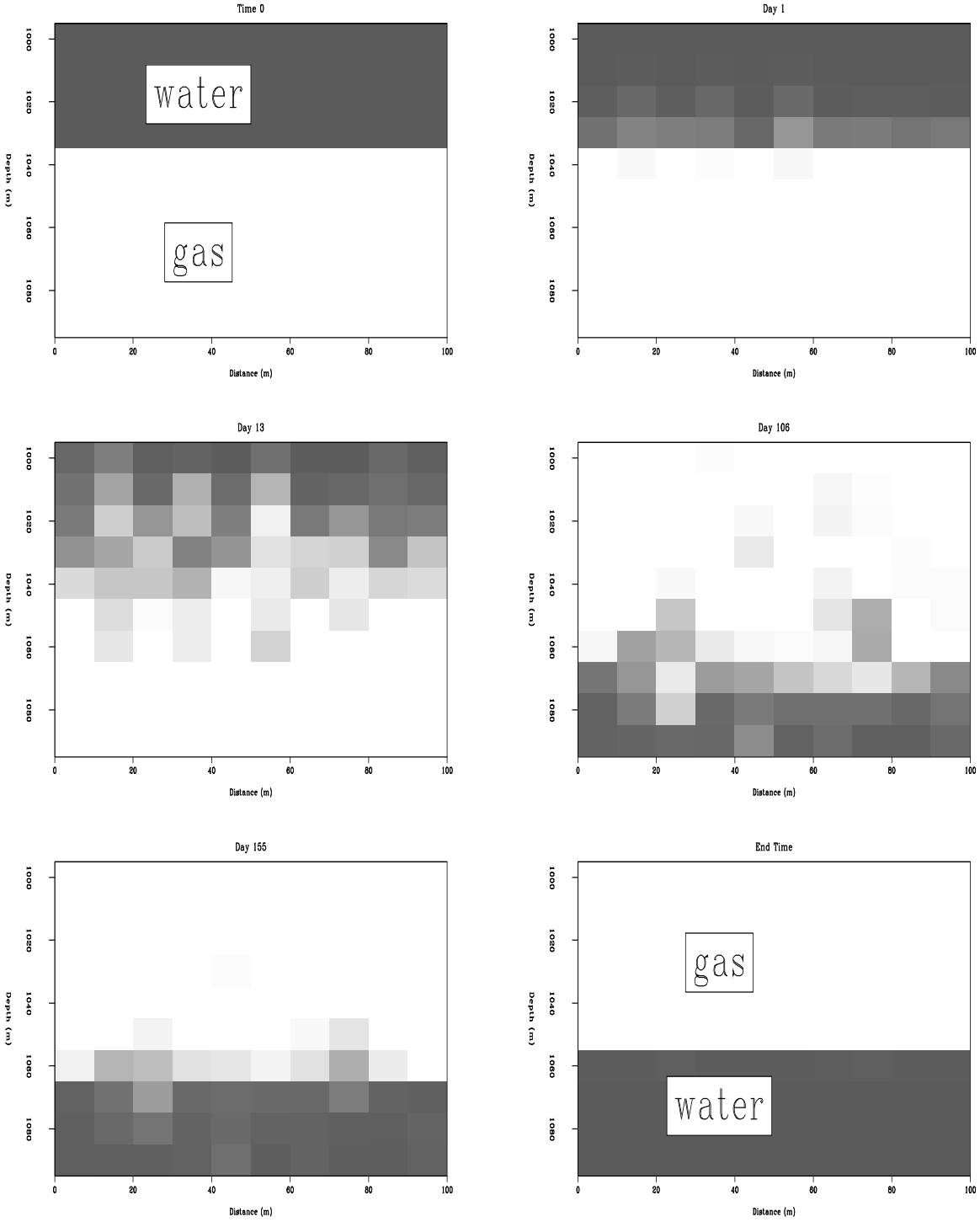

Figure 5: Fluid flow stimulation by an instable system of water over gas. Results are shown for the gas saturation. 100 % gas saturation is displayed as white, 0 % as black. christin1-gaswater-ann [NR]

FUTURE THERMAL EXPANSION

The simplified first assumption of isothermal fluid flow for hydrate structures will not be sufficient for a realistic model of the complex gas-water-hydrate system. The decomposition and growth of hydrate involves complicated thermal effects which have to be included into the fluid-flow simulation. Once the isothermal setup has been improved and is working properly, this can be achieved by extending the system with one more equation. The thermodynamics will be included based on the conservation of energy:

$$\begin{pmatrix} Rate\,of \\ accumulation\,of \\ energy\,in\,V \end{pmatrix} = \begin{pmatrix} Net\,Rate\,of \\ energy\,transported \\ into\,V \end{pmatrix} + \begin{pmatrix} Rate\,of \\ energy\,production \\ in\,V \end{pmatrix}$$

Following this equation of energy balance, the additional fluid flow equation including thermodynamics can be written as:

$$\frac{\partial}{\partial t}\left(\phi \sum_{j=1}^{np} \rho_j S_j U_j + (1-\phi)\rho U - \phi g z \sum_{j=1}^{np} \rho_j S_j + \frac{1}{2}\sum_{j=1}^{np} \rho_j |v_j|^2\right)$$

$$+\nabla\left(\sum_{j=1}^{np} \rho_j v_j (H_j + \frac{1}{2}|v_j|^2 + gz)\right) - \nabla(K\nabla T) = 0 \qquad (31)$$

The number of phases np will be given by gas, water and hydrate. The internal energy of each phase j is denoted by U_j, and the enthalpy is given by H_j. This equation will have to be added to the previous three flow equations in order to include the temperature effects on the gas-water-hydrate structure.

CONCLUSIONS

I have discussed the theory relevant for a three phase/two component isothermal gas-water-hydrate fluid flow simulation of hydrate growth and dissociation. Furthermore, I have shown the finite-difference code development for the three dimensional flow problem. The code has been implemented for two dimensions and is currently running correctly in the case of two-phase gas-water flow, with negligible small hydrate saturation for pressures and temperatures that prevent both hydrate growth or dissociation. I have shown the results of a test case simulating the equilibrization of a water over gas system with time. Also, I have discussed the possible future extension of the code to include thermodynamic effects that are crucial in regard to hydrate structures.

ACKNOWLEDGMENTS

I would like to thank David Lumley for his initial suggestion of hydrate flow simulation. I would also like to thank Marco Thiele and Jack Dvorkin for many helpful discussions and suggestions.

REFERENCES

Aziz, K., 1995, Notes for petroleum reservoir simulation: Stanford University.

Bondarev, E. A., Maksimov, A. M., and Tzypkin, G. C., 1989, Mathematical modeling of the dissociation of gas hydrates: Trans. USSR Acad. Sci. Earth Sci. Sec., **308**, 17–20.

Dallimore, S. R., and Collett, T. S., 1995, Intrapermafrost gas hydrates from a deep core hole in the Mackenzie Delta, Northwest Territories, Canada: Geology, **23**, 527–530.

Dillon, W. P., Lee, M. W., Fehlhaber, K., and Coleman, D. F., 1993, Gas hydrates on the atlantic continental margin of the united states - controls on concentration: The Future of Energy Gases, U.S. Geo. Surv. Prof. paper 1570.

Ecker, C., and Lumley, D. E., 1994, Seismic AVO analysis of methane hydrate structures: 64th Ann. Internat. Meeting, Soc. Expl. Geophys., Expanded Abstracts, 1100–1103.

Ecker, C., Dvorkin, J., and Nur, A., 1995, Sediments with gas hydrates: Internal structure from seismic AVO: SEP–**89**, 1–24.

Englezos, P., Kalogerakis, N., Dholabhai, P. D., and Bishnoi, P. R., 1987, Kinetics of formation of methane and ethane gas hydrates: Chem. Eng. Sci., **42**, 2647–2658.

Jamaluddin, A. K. M., Kalogerakis, N., and Bishnoi, P. R., 1989, Modelling of decomposition of a synthetic cor of methane gas hydrate by coupling intrinsic kinetics with heat transfer rates: Can. Jour. Chem. Eng., **67**, 948–954.

Katzman, R., Holbrook, W. S., and Paul, C. K., 1994, Combined vertical-incidence and wide-angle seismic study of a gas hydrate zone, Blake Ridge: J. Geophys. Res., **99**, 17975–17995.

Kim, H. C., Bishnoi, P. R., Heidemann, R. A., and Rizvi, S. S. H., 1987, Kinetics of methane hydrate decomposition: Chem. Eng. Sci., **42**, 1645–1653.

Kvenvolden, K. A., and Barnard, L. A., 1983, Gas hydrates of the Blake Outer Ridge, Site 533, Deep Sea Drilling Project Leg 76: Initial Reports of the Deep Sea Drilling Project, **76**, 353–365.

Kvenvolden, K., 1993, Gas hydrates – geological perspective and global change: Reviews of Geophysics, **31**, 173–187.

MacKay, M. E., Jarrard, R. D., Westbrook, G. K., and Hyndman, R. D., 1994, Origin of bottom-simulating reflectors : Geophysical evidence from the Cascadian accretionary prism: Geology, **22**, 459–462.

Singh, S., Minshull, T. A., and Spence, G., 1993, Velocity structure of a gas hydrate reflector: Science, **260**, 204–207.

Verigin, N. N., Khabullin, I. L., and Khalikiv, G. A., 1980, Linear problem of the dissociation of the hydrates of a gas in a porous medium: Izvest. Akad. Nauk. SSR, Mekhanika Gaza, **1**, 144–147.

Yousif, M. H., Abass, H. H., Selim, M. S., and Sloan, E. D., 1991, Experimental and theoretical investigation of methane-gas-hydrate dissociation in porous media: SPE Res. Eng., pages 69–76.